International Journal of Engineering

Process Parameter Optimization of 3D-Printer Machine Using Response Surface Method for Printing Hydroxyapatite/Collagen Composite Slurry

N. Nurbaiti[a,b], A. E. Tontowi*[a], M. G. Widyastuti[c], H. V. Hoten[a,b], F. Ibrahim[a], N. Muna[a], R. Febrian[a], D. P. Perkasa[d], M. K. Herliansyah[a]

[a] Mechanical and Industrial Engineering Department, Universitas Gadjah Mada, Yogyakarta, Indonesia
[b] Mechanical Engineering Department, Bengkulu University, Indonesia
[c] Oral and Maxillofacial Surgery Department Gadjah Mada, Yogyakarta, Indonesia
[d] National Nuclear Energy Agency, Indonesia

PAPER INFO

A B S T R A C T

Nowadays, various 3D-Printer technologies are commercially available. However, those printers could only be used for a certain material provided by the printer manufacturers. For new material, the commercial printer could not be employed directly and needs to be modified and its printing parameter has to be optimized to fit the property of the new material. This paper aimed to find the optimum parameters (print speed and layer height) based on printability material. The new material that would be developed was a composite of bioceramic powder (hydroxyapatite) and polymer (collagen) in the form of slurry with ratios of 99.84% (w/v) and 0.16% (w/v). While the printer was a commercial 3D-Printer machine with modification on its cartridge container and bracket. The printing parameters were layer height (0.65, 1.0, 1.35 mm) and print speed (14.4, 25, 35.6 mm/min). Optimization of the printing parameter used Response Surface Method (RSM) with 13 sets of specimens. Test specimens for defining printable material were printed in the form of line shape and a rectangular shape for case study. Printability as a responding of the optimum parameter setting was defined on the basis of 5%-maximum dimension error of the printed specimen compared to the 3D-CAD data. Data obtained was analyzed using ANOVA. The results show that the optimum setup printing parameter were 10.009 mm/min for print speed and 0.505 mm for layer height, respectively with the error dimension obtained from the experiment was 0.013 mm^2 (0.59%) lower than that of the permitted error of 5% (0.125 mm^2).

doi: 10.5829/ije.2023.36.11b.02

NOMENCLATURE

ξ_i	Natural Variable	T_L	Target length (mm)	
Y	First-order response surface model	W	Width (mm)	
β	Intercept	T_W	Target width (mm)	
x	Independent variables	H	Height (mm)	
ε	Error	T_H	Target height (mm)	
L	Length (mm)			

1. INTRODUCTION

Biomaterials have a major impact to improve the quality life of many patients through of functional restorations engineering of body tissues [1]. The requirement of biomaterials are non-carcinogenic nature, non-pyrogenic, non-toxic, absolutely blood compatible, and non-inflammatory [2]. One of the biomaterials purposes is used for biomedical applications and their condition can interact with live body tissues. Metals, ceramics, composites and polymers are classified as biomaterials [3]. Metals like stainless steel, titanium and magnesium alloys are used for biomaterials. However, they have

*Corresponding Author Email: alvaedytontowi@ugm.ac.id (A. E. Tontowi)

some drawbacks such as toxic ions, inflammatory, allergic reactions, and high modulus [4].

Hydroxyapatite (HA) is one such bioceramic that has bioactive properties [5]. It has, thromboresistance, chemical inertia, and physical characteristics similar to bone. HA has a similar composition to bone minerals and excellent biocompatibility; therefore, widely used as a bone substitute [6–8]. However, synthetic HA is brittle, rigid, has low solubility, and poor processability [9, 10]. Moreover, the biodegradation time of HA is 130 months after implantation [11]. Collagen is a natural polymer providing favorable biological conditions. It stimulates the generation and differentiation of cells as an extracellular matrix [12] but they have poor mechanical properties [13]. Combining bioceramic (HA) and polymer (collagen) will overcome the drawback of them. This composite improves mechanical and biological properties, such as resistance to failure [14–17]. Structure of collagen resembles a rope, triple helix, high strength, and tensile strength [18]. Research and commercial studies of composites HA/collagen began around the 1980's [19].

Additive manufacturing techniques allow the construction of objects point by point, line by line, or layer by layer [20, 21]. There are two basic steps of 3D printing. Firstly the object design via computer software and secondly, the object deposition/ formation via a 3D printer [22]. The International Organization for Standardization (ISO) and American Society for Testing and Materials (ASTM) classify 3D printing technologies into seven different categories, namely binder jetting (BJ), direct energy deposition, material extrusion, Material Jetting, Powder Bed Fusion, Sheet Lamination, and Photopolymerization [4]. Three dimensional printing technology using slurry was explained by Lin et al. [23] and Putlyaev et al. [24]. Lin et al. [23] described using stereolithography and direct ink writing for slurry ceramic. Ceramic slurry for stereolithography should have long-term stability and suitable rheological behavior to enable a smooth flow for printing and homogeneity of the printed part. In terms of viscosity, the slurry has to be ideally comparable to the resin (<3000 mP·s). In contrast, Direct Ink Writing (DIW) is more economical and faster, including fabrication, drying, and sintering. However, the challenge is after the extrusion process such as crack happens.

Putlyaev et al.[24] produced bioceramic scaffolds using stereolithographic 3D printing of light-cured slurries containing a mixed calcium sodium phosphate $Ca_{2.5}Na(PO_4)_2$ composition. Extrusion-based bioprinting is 3D printing that is widely used to print organs. This is related to rheological properties [25].

The science that studies the deformation and flow of materials is called rheology [26]. Material rheology is related to cell behavior. It correlates between particle mobility and cell speed across length scales [27].

Characterization of rheology is important to the design of concentrated dispersions of ceramic particles (also called slurries). Furthermore, the rheological properties of these viscoelastic fluids determine in which ways these formulations can be utilized or further processed. However, in the biomaterials research field, the rheology of ceramic formulations is often treated neglectfully thought of the complexities involved [28].

Design of experiment (DoE) as a collection of data is adopted by RSM [29]. RSM was introduced by Box and Wilson in 1951 [30, 31]. It is useful not only in the engineering sector but also in a variety of other fields [32]. It is the best combination of mathematical and statistical techniques for non-linear relationships among multi-objective inputs, their response, and to predict multivariant optimization. It is necessary because the sample point must be chosen to create a credible model with the fewest feasible tests [33, 34].

The main advantage of RSM is the decreased required number of experimental runs in predicting the optimum state compared to other optimizing techniques and avail a systematic, satisfactory result compared to the one-factor model [32, 35–37]. It is principally based on the fit of practical equations on experimental data determined from the given design [38]. It employs linear and polynomial equations (quadratic, cubic, or higher-order functions). RSM offers a unique capability for developing an empirical link between factor variables and experimental design procedure responses [39].

The purpose of this research was to get the printability and optimum parameter process of 3D-printer machine using response surface method for printing (HA/collagen) composite slurry.

2. METHODS

2. 1. Materials HA 04238 type (density 1.0 g/cm³, molecular weight 502.31 g/mol, density 1.0 g/cm³ at 20 °C) was purchased from Sigma Aldrich and collagen which is synthesis from mackerel (Scomberomous SP) skin that was used as raw materials. Characterization of collagen with amino acid analysis using High Performance Liquid Chromatography (HPLC) with Thermo Dionex UltiMate 3000 in the Organic Chemistry Laboratory, Faculty of Mathematics and Natural Sciences, Universitas Gadjah Mada. The concentrations of the amino acids of the collagen (in ppm) are aspartic acid 41.68, glutamicacid 71.28, serine 22.47, glycine 103.93, threonine 19.61, arginine 65.05, alanine 62.44, tyrosine 12.20, methionine 10.80, valine 18.44, phenylalan in 21.16, ileucine 13.60, leucine 21.83, and lysine 34.95. The solvents used acetic acid (glacial 100%) to dissolve (HA/collagen) composite and Sodium Hydroxide to balance pH, which was purchased from Sigma Aldrich.

2. 2. Material Preparation

Preparation of (HA/collagen) composite slurry collagen was carried out by dissolving collagen in acetic acid solution (pH=2) at low concentration of 0.2% (w/v) and stirring for 30 minutes. HA powder was mixed gradually into the collagen solution with ratio of 99.84% (w/v) and 0.16% (w/v). During mixing, stirring using magnetic stirrer was carried out for the first step from 250 rpm to 800 rpm and stirring was continued by hand stirring to form slurry composite. To adjust pH, Sodium Hydroxide 0.4 M (pH=14) was used. The slurry composite was kept at room temperature.

2. 3. 3D-Bioprinter System

A modified 3D-Bioprinter was used for printing specimens. This 3D printer machine was a commercial machine (Eazao Zero type, Qingdao Eazao Intelligent Technology Co., Ltd., China) (Figure 1). Modification has been carried out on the cartridge container and bracket in order to fit to the limited use of slurry composite materials. The nozzle was a hollow needle with diameter of 1.5 mm.

2. 4. Specimen Preparation

Two types of printed specimens were used in this research. First was specimens in the form of a line shape for defining printable material and second was a rectangular shape for a case study. The dimensions of line were 20 mm long x 1.5 mm wide x 1.5 mm height. While, the dimensions of rectangular shape were 20 mm long x 20 mm wide x 5 mm height. The height of the rectangular specimen was composed by several layer of line. The dimensions of printing line and rectangular specimen are shown in Figure 2. All specimens were printed following the Design of Experiment.

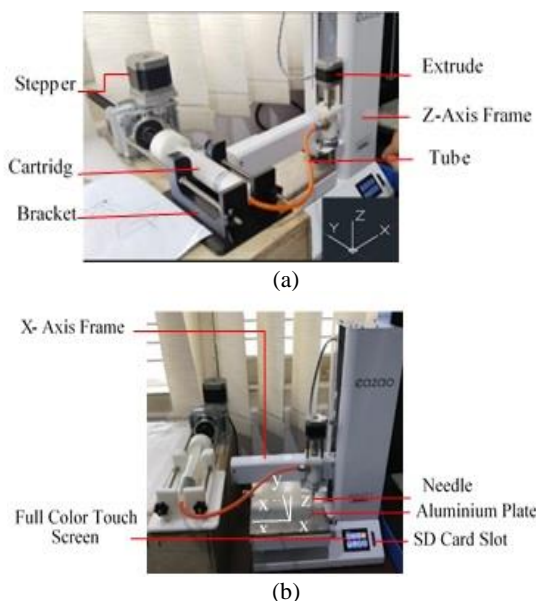**Figure 1.** (a) and (b) 3D bioprinter based on slurry extrusion
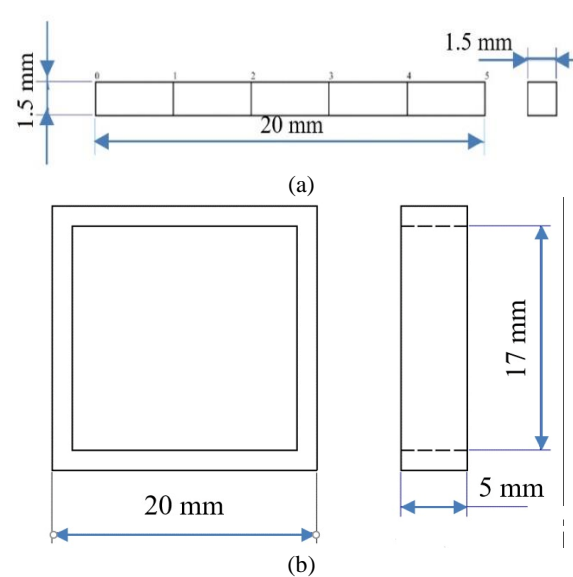
Figure 2. The dimensions of specimens (a) line (b) rectangular

The printing process begins with leveling of the aluminium table plate of the machine. The gap between upper surface of the table and edge of nozzle/needle was set up of 0.1mm. Next, the slurry was transferred from the mixing container into the cartridge using a micro spatula and ready for printing. On the touch screen, select the back putter (out) menu. In this, piston within the cartridge will push the slurry material into the plastic air tubing, enter to the extruder and the material comes out through the needle. Select the file of specimen that has been prepared and press the print menu. The percentage of composite slurry material was 1% (in the range of 1%-10%). Data of printed specimens was gathered by measuring dimension of specimen using a MiViewCap microscope.

2. 5. Printability and Optimization Method

Optimization of printing parameter process is important for obtaining printability. For the 3D bioprinter there are five printing parameter process including ambient temperature, nozzle diameter, flow rate, print speed, and layer height. The ambient temperature was set up at room temperature and diameter nozzle is 1.5 mm. The flow rate of the slurry from the nozzle was 10 mm³/s. In this study only print speed and layer height were optimized as printing process parameters. While, the ambient temperature, nozzle diameter and flow rate were set up as fixed value. To determine the optimum parameters, each parameter had to be set into three levels and two factors as described in Table 1. The two factors include A: Print Speed (mm/min) and B: layer height (mm) with coded levels high (+1), low (−1), and center points (0). The actual values of the print speed representing levels were 14.4, 25, and 35.6 mm/min. While, the layer height

TABLE 1. Factor and level used based on the standard in the Eazao Zero machine

Factor	Level		
	-1	0	+1
A: Print Speed (mm/min)	14.4	25	35.6
B: Layer Height (mm)	0.65	1	1.35

representing levels were 0.65, 1, 1.35 mm. These values were taken from the data sheet specification of Eazao Zero machine. The print speed was between 10 - 40 mm/min. While the layer height was between 0.5 - 1.5 mm.

The range of each level was obtained through the Coded Value Equation [40]. The equation of coded value is as Equation (1):

$$x_i = \frac{\xi_i - (\frac{high+low}{2})}{(\frac{high-low}{2})} \tag{1}$$

In this study, there are two factors so it uses the central composite design that is shown in Figure 3.

Figure 3 shows 2^2 designs with four axial runs. The maximum and minimum values of the print speed are 35.6 mm/s and 14.4 mm/s while the layer height are 1.35 mm and 0.65 mm.

Based on the Central Composite Design (2 levels), 13 observations were obtained as shown in Table 2.
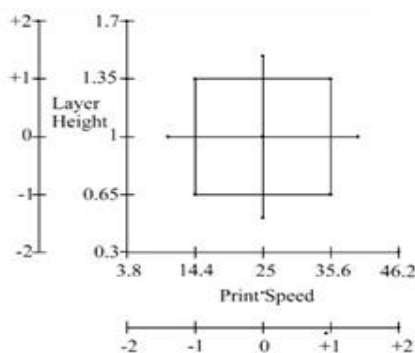
Figure 3. Central Composite Design

TABLE 2. Design of experiment (DoE)

No	Coded Variable		Actual Variable	
	Print Speed	Layer Height	A	B
1	0	0	25	1
2	-1.414	0	10.009	1
3	1.414	0	39.99	1
4	0	0	25	1
5	-1	1	14.4	1.35
6	0	0	25	1
7	0	0	25	1
8	-1	-1	14.4	0.65
9	0	-1.414	25	0.505
10	0	0	25	1
11	1	1	35.6	1.35
12	1	-1	35.6	0.65
13	0	1.414	25	1.494

Printability is defined as the ability to form and preserve reproducible using 3D printing from bioink material [41]. The printability test is carried out by printing line with 3D bioprinter based on slurry extrusion. The DoE was used for the dimensional error test. Each printed product from each parameter will be separated into 5 areas in the X, Y and Z directions. Then these values were compared with the dimension on the CAD drawings. Dimensions measured were in the wet conditions of the specimen. The result was calculated by the sum of multiplication between different dimensions and the target in the form of width and height. Furthermore, the average and percentage of error dimensions were determined. It is printable when it has a dimensional error of no more than 5%.

Optimization was obtained using RSM with Minitab 18 software for getting optimum parameters of the print speed and layer height that are started by doing first-order tests. The RSM regression model is generally quadratic full equation or reduced form [42]. This test is calculated by the following mathematical Equation (2) (RSM equation):

$$Y = \beta_0 + \beta_1 x_1 + \beta_2 x_2 + \beta_{11} x_1^2 + \beta_{22} x_2^2 + \beta_{12} x_1 x_2 + \varepsilon \tag{2}$$

Moreover, a lack of fit test is carried out to identify the type of error that occurred. Data is valid and normally distributed when the p-value is greater than α otherwise data is not valid and not normally distributed when the p-value is less than α. The difference between the proposed model and the experimental data can be calculated using dimensional error and a mathematical model will be obtained. Furthermore, the results will be analyzed using the Analysis of Variance (ANOVA). Finally, the interaction between these parameters will be obtained which shows the optimum results for each interaction. Validation can be carried out by comparing the dimensional error result in RSM based on Equation (2) and the dimensional error from the experiment.

3. RESULTS AND DISCUSSION

Based on the design of the experiment HA/collagen composites were printed using 13 sets of specimens.

Specimens are illustrated in Figure 4. As Figure 4 shows the printability material composite HA/Collagen. Printability and dimensional error from the experiment are shown in Table 3 and Figure 5.

Table 3 shows the error dimensions for 13 sets of specimens from 13 parameters. Parameters 8 and 9 have allowable error limits. Their respective values are 0.104 mm^2 (4.61%) and 0.085 mm^2 (3.76%). In this study, the maximum allowable limit value is 0.1125 mm^2 (5%).

Figure 5 shows the printability of material composite. Parameters 8 and 9 are printable. Parameter 9 is the most printable. Positive value indicates the average surface dimensional error of the five specimen points exceeds the surface dimension size of the CAD drawing. This means that there is deformation that occurs between one layer and the next layer in the wet condition. Conversely, a negative value indicates an error its surface dimension shrinks compared to the CAD drawing surface.

The Analysis of Variance (ANOVA) is tested to determine whether the error occurs systematically or not. After the ANOVA test, the primary effect parameter analysis is carried out, which has the most significant influence. It shows in Table 4.

**TABLE 3**. Dimensional error for 13 sets of specimens

Actual Variable	Dimensional Error (mm²)	The mean of Dimensional error (mm²)	Percentage of dimensional error (%)	Actual Variable
A	B			
25	1	1.988	0.398	17.67
10.009	1	1.852	0.370	16.46
39.99	1	3.901	0.780	34.68
25	1	3.845	0.769	34.18
14.4	1.35	-3.262	-0.652	28.99
25	1	4.275	0.855	38.00
25	1	2.742	0.548	24.37
14.4	0.65	-0.519	-0.104	4.61
25	0.505	-0.423	-0.085	3.76
25	1	2.430	0.486	21.60
35.6	1.35	-3.187	-0.637	28.33
35.6	0.65	2.788	0.558	24.79
25	1.494	-1.769	-0.354	15.72

TABLE 4. ANOVA for print speed and layer height

Source	DF	Adj SS	Adj MS	F-Value	P-Value
Model	5	13.151	2.6301	4.18	0.044
Linear	2	6.446	3.223	5.12	0.043
A	1	3.249	3.249	5.16	0.057
B	1	3.196	3.196	5.08	0.059

Square	2	5.348	2.674	4.25	0.062
A²	1	0.0039	0.0039	0.01	0.939
B²	1	5.2168	5.2168	8.28	0.024
2-way Interaction	1	1.374	1.374	2.18	0.183
A*B	1	1.374	1.374	2.18	0.183
Error	7	4.408	0.629		
Lack-of-Fit	3	0.668	0.223	0.24	0.866
Pure Error	4	3.739	0.935		
Total	12	17.558			

(a)
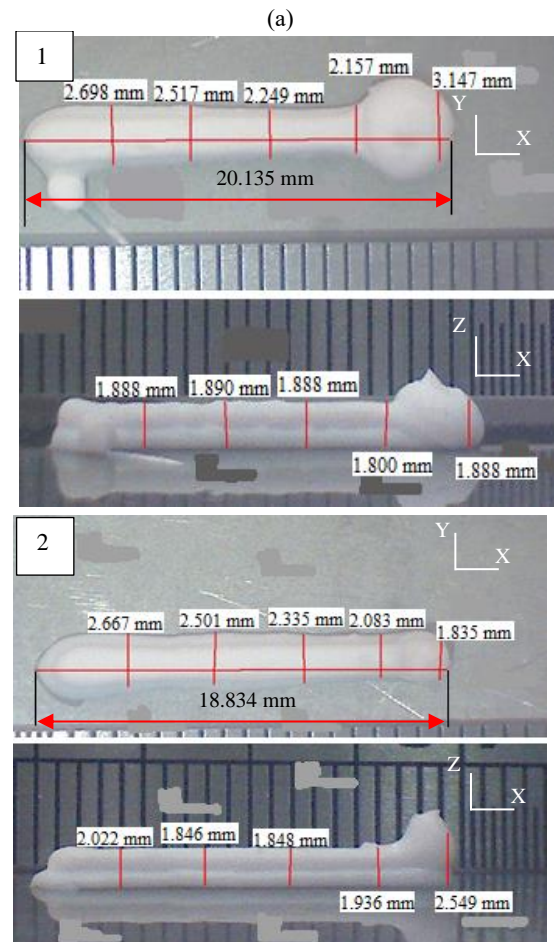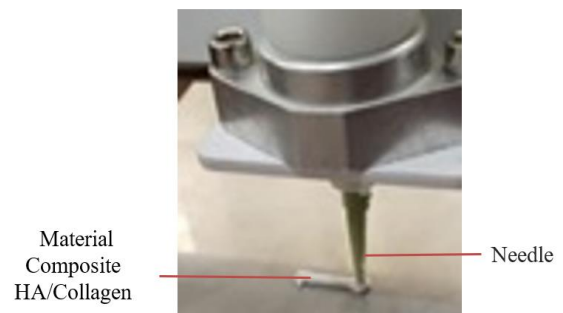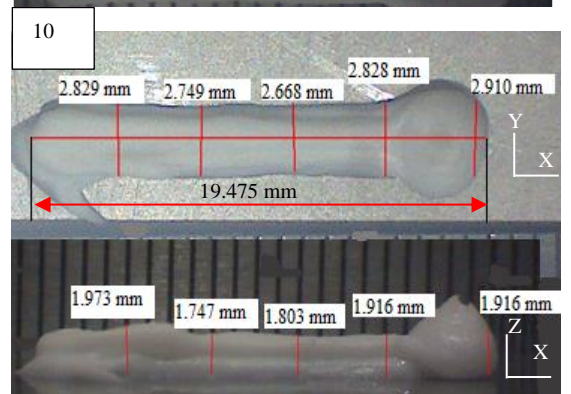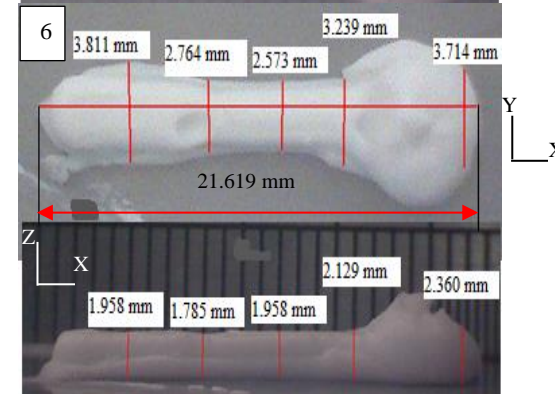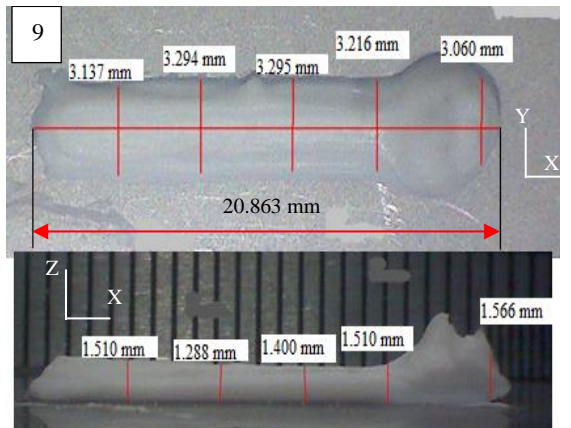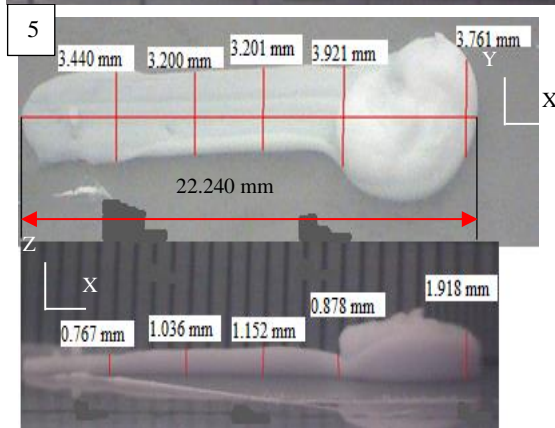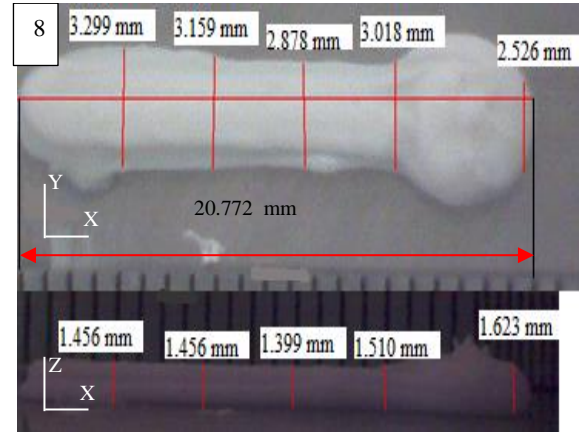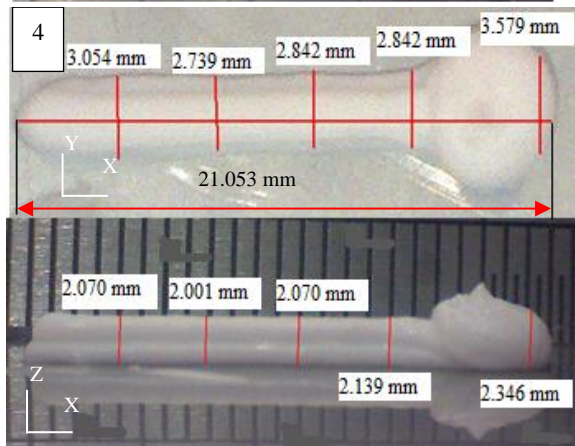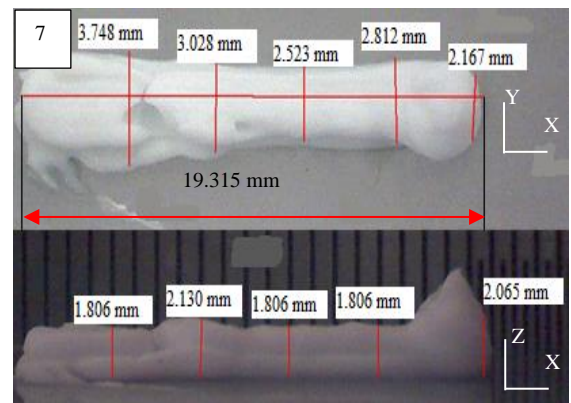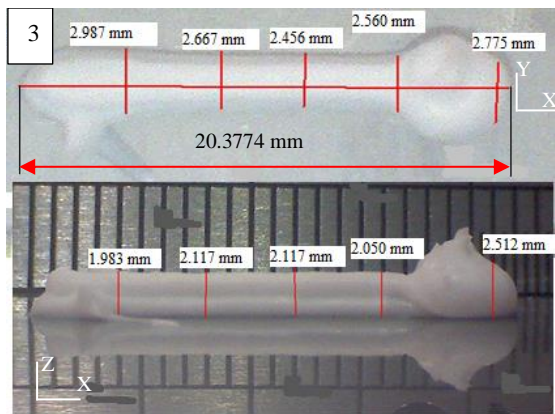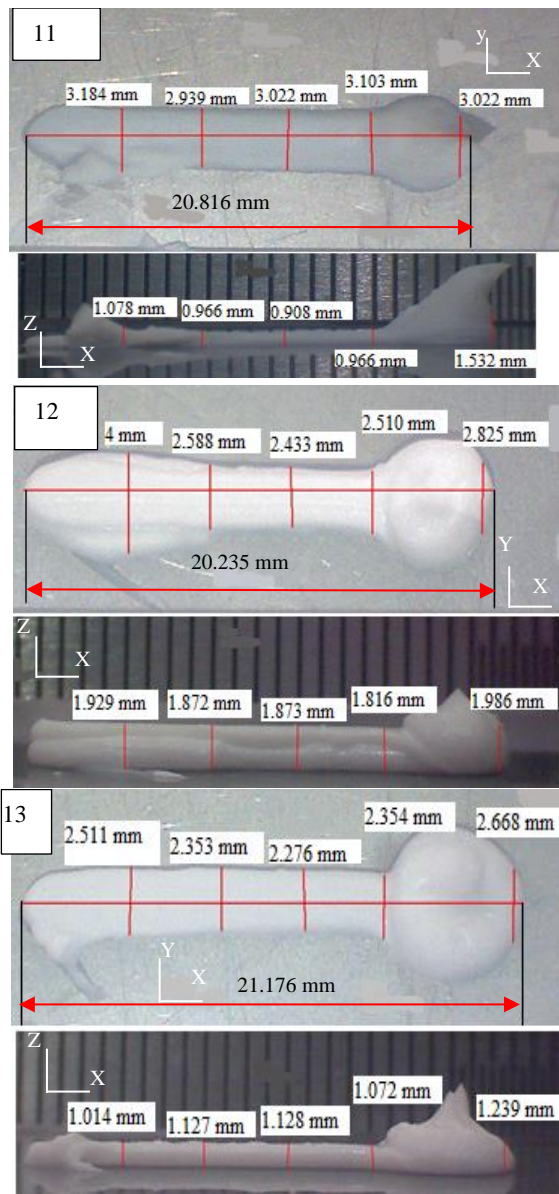
Figure 4. (a) 3D printing process. (b) printing for 13 sets of specimens
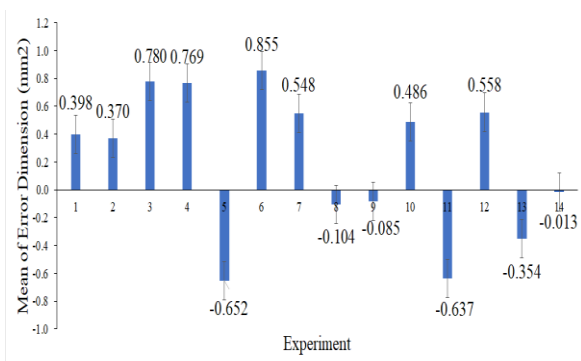
Table 4 shows a lack of fit value of 0.866, which means that it is greater than the α value for the confidence interval 95% (α=5%) so that the model used (which is estimated based on data) is suitable for a relationship between variables. Moreover, the parameter that has a significant effect is the quadratic layer height because it has p-value smaller than the α value. Regarding these interactions, the regression model Equation (3) is obtained.

$$Yg = -7.33 + 0.06A + 16.01B - 7.108B^2 \qquad (3)$$

The effect parameters process on response can be presented in a Pareto chart as shown in Figure 6.

Figure 6 shows the effect of layer height quadratically is the most influential dimensional error. The interaction of two same parameters also has an effect. This indicates that the relationship between the parameters and the dimensional error response follows a curved line or is not linear.

Figure 7 shows the effect parameters machine versus error dimension. A linear curve was shown between print speed and dimensional error. It means that print speed increases when the dimensional error increases. Contrarily, the error dimension will decrease if the print speed is lowered. Furthermore, layer height and error dimension form a parabolic curve. Layer height increases then the dimensional error that occurs will increase until it reaches the maximum point (about 1.12 mm). It means that the dimensional error maximum for 13 parameters is 1.12 mm. After that, the dimension error will decrease even though the layer height increased to 1.5 mm.

It is necessary to obtain the optimum value of each of these parameters based on the interaction between them. The surface plot of the interactions between these parameters are illustrated in Figure 8. Moreover, optimum parameter results are shown in Figure 9.

Figure 9 shows the results of the analysis optimum values for the process parameters (print speed and layer height) are 10.009 mm/min and 0.5050 mm, respectively.
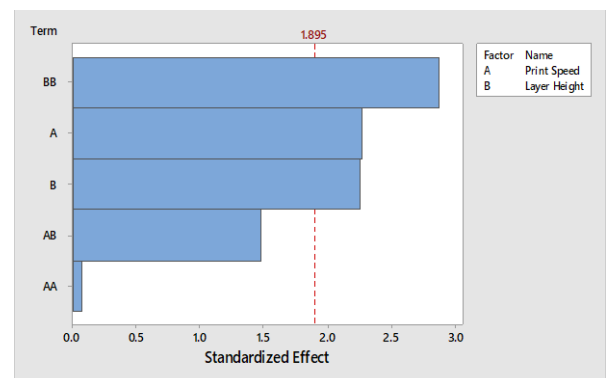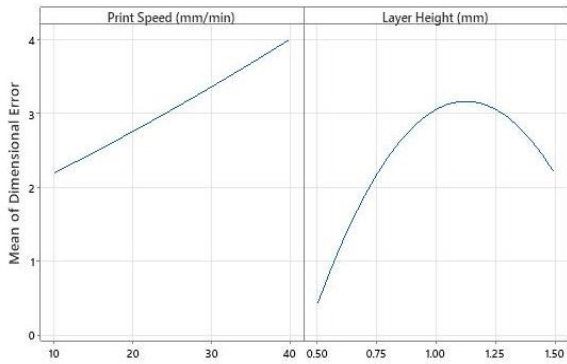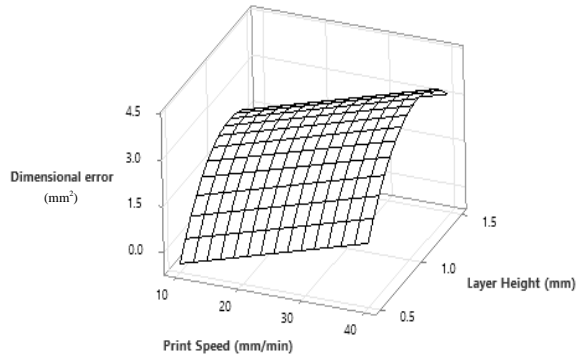

Figure 5. Printability test for 13 sets of specimens

Figure 6. Pareto Chart between Print Speed and Layer Height versus Dimensional Error

Figure 7. The effect of 3D Printer parameters machine versus error dimension


**Figure 8.** Surface Plot Print Speed and Layer Height versus Dimensional Error

Dimensional error results using these optimum parameters from analysis with a value of -1.5994 mm^2.

Print composite materials using the optimum parameters is shown in Figure 10 in line.
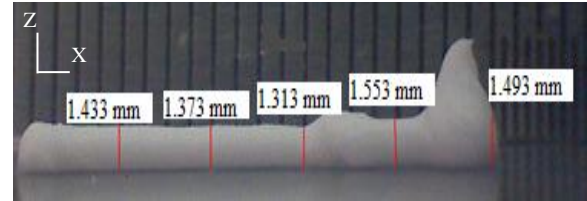
Figure 10a shows the print results in line product. Figure 10b shows five points with the same scale on the Y and Z axes. The mean dimensional error is 0.013 mm^2 (0.59%). Part product for the case study is shown in Figure 11.
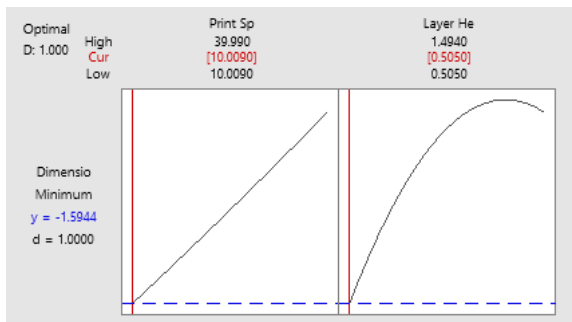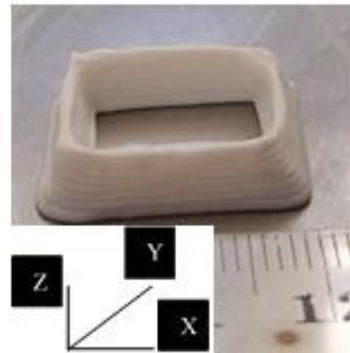

Figure 9. Optimum parameter results
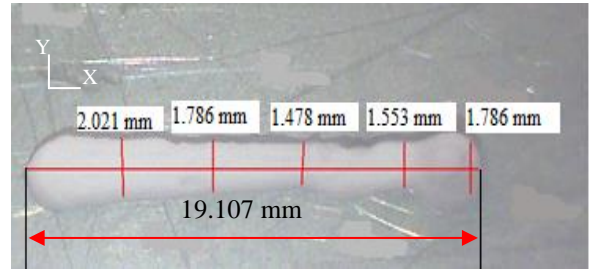
Figure 10. (a) Printing of line product dimension in the Y axis (b) dimension in the Z axis

Figure 11. Product using optimum parameters

4. CONCLUSION

Optimum parameter process of 3D printer machine for printing (hydroxyapatite/collagen) composite slurry was successfully obtained. Composite slurry (hydroxyapatite/collagen) was prepared with ratios of 99.84% (w/v) and 0.16% (w/v). The printing process was carried out using commercial machine (3D printer Eazao Zero) with modified cartridge and bracket because composite slurry is used in limited quantities. There are two parameters used in this study namely print speed and layer height with 13 set specimens. The optimum process parameter values for print speed and layer height were 10.009 mm/min and 0.505 mm, respectively. Furthermore, the printability test shows a dimensional error of the optimum parameter of about 0.013 mm^2 (percentage of error dimension 0.59%). Regarding the result, it is printable because of the permissible error limit of 5% (0.013 mm^2).

5. ACKNOWLEDGEMENTS

6. REFERENCES

1. Ronoh, K., Mwema, F., Dabees, S., and Sobola, D. "Advances in sustainable grinding of different types of the titanium biomaterials for medical applications: A review." *Biomedical Engineering Advances*, Vol. 4, (2022), 100047. https://doi.org/10.1016/J.BEA.2022.100047

2. Agarwal, K. M., Singh, P., Mohan, U., Mandal, S., and Bhatia, D. "Comprehensive study related to advancement in biomaterials for medical applications." *Sensors International*, Vol. 1, (2020), 100055. https://doi.org/10.1016/J.SINTL.2020.100055

3. Ajmal, S., Athar Hashmi, F., and Imran, I. "Recent progress in development and applications of biomaterials." *Materials Today: Proceedings*, Vol. 62, (2022), 385-391. https://doi.org/10.1016/J.MATPR.2022.04.233

4. Kanwar, S., and Vijayavenkataraman, S. "Design of 3D printed scaffolds for bone tissue engineering: A review." *Bioprinting*, Vol. 24, (2021), e00167. https://doi.org/10.1016/J.BPRINT.2021.E00167

5. Annur, D., Bayu, F., Supriadi, S., and Suharno, B. "Electrophoretic Deposition of Hydroxyapatite/Chitosan Coating on Porous Titanium for Orthopedic Application." *Evergreen*, Vol. 9, No. 1, (2022), 109-114. https://doi.org/10.5109/4774222

6. Kumar, M., Ghosh, S., Kumar, V., Sharma, V., and Roy, P. "Tribo-mechanical and biological characterization of PEGDA/bioceramics composites fabricated using stereolithography." *Journal of Manufacturing Processes*, Vol. 77, (2022), 301-312. https://doi.org/10.1016/J.JMAPRO.2022.03.024

7. Tontowi, A. E., Raharjo, K. P., Sihaloho, R. I., and Baroroh, D. K. "Comparison of design method for making composite of (PMMA/HA/Sericin)." *Materials Science Forum*, Vol. 901 MSF, (2017), 85-90. https://doi.org/10.4028/www.scientific.net/MSF.901.85

8. Van Hoten, H., Gunawarman, Mulyadi, I. H., Mainil, A. K., Bismantolo, P., and Nurbaiti. "Parameters optimization in manufacturing nanopowder bioceramics of eggshell with pulverisette 6 machine using taguchi and ANOVA method." *International Journal of Engineering, Transactions A: Basics*, Vol. 31, No. 1, (2018), 45-49. https://doi.org/10.5829/ije.2018.31.01a.07

9. You, B. C., Meng, C. E., Mohd Nasir, N. F., Mohd Tarmizi, E. Z., Fhan, K. S., Kheng, E. S., Abdul Majid, M. S., and Mohd Jamir, M. R. "Dielectric and biodegradation properties of biodegradable nano-hydroxyapatite/starch bone scaffold." *Journal of Materials Research and Technology*, Vol. 18, (2022), 3215-3226. https://doi.org/10.1016/J.JMRT.2022.04.014

10. Bhat, S., Uthappa, U. T., Altalhi, T., Jung, H. Y., and Kurkuri, M. D. "Functionalized Porous Hydroxyapatite Scaffolds for Tissue Engineering Applications: A Focused Review." *ACS Biomaterials Science and Engineering*, (2021). https://doi.org/10.1021/acsbiomaterials.1c00438

11. Ou, M., and Huang, X. "Influence of bone formation by composite scaffolds with different proportions of hydroxyapatite and collagen." *Dental Materials*, Vol. 37, No. 4, (2021), e231-e244. https://doi.org/10.1016/J.DENTAL.2020.12.006

12. Arahira, T., and Todo, M. "Development of novel collagen scaffolds with different bioceramic particles for bone tissue engineering." *Composites Communications*, Vol. 16, (2019), 30-32. https://doi.org/10.1016/J.COCO.2019.08.012

13. Ambekar, R. S., and Kandasubramanian, B. "Progress in the Advancement of Porous Biopolymer Scaffold: Tissue Engineering Application." *Industrial and Engineering Chemistry Research*, Vol. 58, No. 16, (2019), 6163-6194. https://doi.org/10.1021/acs.iecr.8b05334

14. Ramesh, N., Moratti, S. C., and Dias, G. J. "Hydroxyapatite–polymer biocomposites for bone regeneration: A review of current trends." *Journal of Biomedical Materials Research - Part B Applied Biomaterials*, Vol. 106, No. 5, (2018), 2046-2057. https://doi.org/10.1002/jbm.b.33950

15. Chai, Y., Okuda, M., Otsuka, Y., Ohnuma, K., and Tagaya, M. "Comparison of two fabrication processes for biomimetic collagen/hydroxyapatite hybrids." *Advanced Powder Technology*, Vol. 30, No. 7, (2019), 1419-1423. https://doi.org/10.1016/J.APT.2019.04.012

16. Mallick, M., Are, R. P., and Babu, A. R. "An overview of collagen/bioceramic and synthetic collagen for bone tissue engineering." *Materialia*, Vol. 22, (2022), 101391. https://doi.org/10.1016/J.MTLA.2022.101391

17. Nemati, N. H., and Mirhadi, S. M. "Study on Polycaprolactone Coated Hierarchical Meso/Macroporous Titania Scaffolds for Bone Tissue Engineering." *International Journal of Engineering, Transactions A: Basics*, Vol. 35, No. 10, (2022), 1887-1894. https://doi.org/10.5829/ije.2022.35.10a.08

18. Sharma, S., Rai, V. K., Narang, R. K., and Markandeywar, T. S. "Collagen-based formulations for wound healing: A literature review." *Life Sciences*, Vol. 290, (2022), 120096. https://doi.org/10.1016/J.LFS.2021.120096

19. Maher, M., Castilho, M., Yue, Z., Glattauer, V., Hughes, T. C., Ramshaw, J. A. M., and Wallace, G. G. "Shaping collagen for engineering hard tissues: Towards a printomics approach." *Acta Biomaterialia*, Vol. 131, (2021), 41-61. https://doi.org/10.1016/J.ACTBIO.2021.06.035

20. Lamnini, S., Elsayed, H., Lakhdar, Y., Baino, F., Smeacetto, F., and Bernardo, E. "Robocasting of advanced ceramics: ink optimization and protocol to predict the printing parameters - A review." *Heliyon*, Vol. 8, No. 9, (2022), e10651. https://doi.org/10.1016/J.HELIYON.2022.E10651

21. Tagliaferri, S., Panagiotopoulos, A., and Mattevi, C. "Direct ink writing of energy materials." *Materials Advances*, Vol. 2, No. 2, (2021), 540-563. https://doi.org/10.1039/d0ma00753f

22. Mohammed, A. A., Algahtani, M. S., Ahmad, M. Z., Ahmad, J., and Kotta, S. "3D Printing in medicine: Technology overview and drug delivery applications." *Annals of 3D Printed Medicine*, Vol. 4, (2021), 100037. https://doi.org/10.1016/j.stlm.2021.100037

23. Lin, K., Sheikh, R., Romanazzo, S., and Iman, R. "3D Printing of Bioceramic Scaffolds — Barriers to the Clinical Translation : From Promise to Reality, and Future Perspectives." *Materials*, Vol. 12, No. 17, (2019), 2660.

24. Putlyaev, V. I., Yevdokimov, P. V., Mamonov, S. A., Zorin, V. N., Klimashina, E. S., Rodin, I. A., Safronova, T. V., and Garshev, A. V. "Stereolithographic 3D Printing of Bioceramic Scaffolds of a Given Shape and Architecture for Bone Tissue Regeneration." *Inorganic Materials: Applied Research*, Vol. 10, No. 5, (2019), 1101-1108. https://doi.org/10.1134/S2075113319050277

25. Zhang, T., Zhao, W., Xiahou, Z., Wang, X., Zhang, K., and Yin, J. "Bioink design for extrusion-based bioprinting." *Applied Materials Today*, Vol. 25, (2021), 101227. https://doi.org/10.1016/J.APMT.2021.101227

26. Lu, C., Zhang, Z., Shi, C., Li, N., Jiao, D., and Yuan, Q. "Rheology of alkali-activated materials: A review." *Cement and Concrete Composites*, Vol. 121, (2021), 104061. https://doi.org/10.1016/J.CEMCONCOMP.2021.104061

27. McGlynn, J. A., Druggan, K. J., Croland, K. J., and Schultz, K. M. "Human mesenchymal stem cell-engineered length scale dependent rheology of the pericellular region measured with bi-disperse multiple particle tracking microrheology." *Acta Biomaterialia*, Vol. 121, (2021), 405-417. https://doi.org/10.1016/J.ACTBIO.2020.11.048

28. Maas, M., Hess, U., and Rezwan, K. "The contribution of rheology for designing hydroxyapatite biomaterials." *Current Opinion in Colloid & Interface Science*, Vol. 19, No. 6, (2014), 585-593. https://doi.org/10.1016/J.COCIS.2014.09.002

29. Ghelich, R., Jahannama, M. R., Abdizadeh, H., Torknik, F. S., and Vaezi, M. R. "Central composite design (CCD)-Response surface methodology (RSM) of effective electrospinning parameters on PVP-B-Hf hybrid nanofibrous composites for synthesis of HfB2-based composite nanofibers." *Composites Part B: Engineering*, Vol. 166, (2019), 527-541. https://doi.org/10.1016/J.COMPOSITESB.2019.01.094

30. Hadiyat, M. A., Sopha, B. M., and Wibowo, B. S. "Response Surface Methodology Using Observational Data: A Systematic Literature Review." *Applied Sciences (Switzerland)*, Vol. 12, No. 20, (2022). https://doi.org/10.3390/app122010663

31. Vahdani, M., Ghazavi, M., and Roustaei, M. "Prediction of mechanical properties of frozen soils using response surface method: An optimization approach." *International Journal of Engineering, Transactions A: Basics*, Vol. 33, No. 10, (2020), 1826–1841. https://doi.org/10.5829/IJE.2020.33.10A.02

32. Singh, D. K., and Tirkey, J. V. "Modeling and multi-objective optimization of variable air gasification performance parameters using Syzygium cumini biomass by integrating ASPEN Plus with Response surface methodology (RSM)." *International Journal of Hydrogen Energy*, Vol. 46, No. 36, (2021), 18816-18831. https://doi.org/10.1016/J.IJHYDENE.2021.03.054

33. Waila, V. C., Sharma, A., and Yusuf, M. "Optimizing the Performance of Solar PV Water Pump by Using Response Surface Methodology." *Evergreen*, Vol. 9, No. 4, (2022), 1151-1159. https://doi.org/10.5109/6625726

34. Reddy, S. S., and Reddy, M. A. K. "Optimization of calcined bentonite caly utilization in cement mortar using response surface methodology." *International Journal of Engineering, Transactions A: Basics*, Vol. 34, No. 7, (2021), 1623-1631. https://doi.org/10.5829/IJE.2021.34.07A.07

35. Sun, W., Feng, L., Abed, A. M., Sharma, A., and Arsalanloo, A. "Thermoeconomic assessment of a renewable hybrid RO/PEM electrolyzer integrated with Kalina cycle and solar dryer unit using response surface methodology (RSM)." *Energy*, Vol. 260, (2022), 124947. https://doi.org/10.1016/J.ENERGY.2022.124947

36. Cao, C., Zhao, Y., Dai, D., Zhang, X., Song, Z., Liu, Q., Liu, G., Gao, Y., Zhang, H., and Zheng, Z. "Simulation analysis and optimization of laser preheating SiC ceramics based on RSM." *International Journal of Thermal Sciences*, Vol. 185, (2023), 108070. https://doi.org/10.1016/J.IJTHERMALSCI.2022.108070

37. Karkare, Y. Y., Sathe, V. S., and Chavan, A. R. "RSM-CCD optimized facile and efficient microwave-assisted green synthesis of Aripiprazole intermediate." *Chemical Engineering and Processing - Process Intensification*, Vol. 173, (2022), 108819. https://doi.org/10.1016/J.CEP.2022.108819

38. Hosseinpour, M., Soltani, M., Noofeli, A., and Nathwani, J. "An optimization study on heavy oil upgrading in supercritical water through the response surface methodology (RSM)." *Fuel*, Vol. 271, (2020), 117618. https://doi.org/10.1016/J.FUEL.2020.117618

39. Isaac, R., and Siddiqui, S. "Sequestration of Ni(II) and Cu(II) using FeSO4 modified Zea mays husk magnetic biochar: Isotherm, kinetics, thermodynamic studies and RSM." *Journal of Hazardous Materials Advances*, Vol. 8, (2022), 100162. https://doi.org/10.1016/J.HAZADV.2022.100162

40. Myer, H. R., Montgomery, C. D., and Anderson-cook, M. C. Response Surface Methodology (Vol. 21). Wiley. Retrieved from http://journal.um-surabaya.ac.id/index.php/JKM/article/view/2203

41. Naghieh, S., and Chen, X. "Printability–A key issue in extrusion-based bioprinting." *Journal of Pharmaceutical Analysis*, Vol. 11, No. 5, (2021), 564-579. https://doi.org/10.1016/j.jpha.2021.02.001

42. Karimi, Y., Rashahmadi, S., and Hasanzadeh, R. "The effects of newmark method parameters on errors in dynamic extended finite element method using response surface method." *International Journal of Engineering, Transactions A: Basics*, Vol. 31, No. 1, (2018), 50-57. https://doi.org/10.5829/ije.2018.31.01a.08
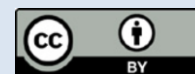
Persian Abstract

چکیده

امروزه فناوری های مختلف چاپگر سه بعدی به صورت تجاری در دسترس هستند. با این حال، این چاپگرها را فقط می‌توان برای مواد خاصی که توسط تولیدکنندگان چاپگر ارائه می‌شد استفاده کرد. برای مواد جدید، چاپگر تجاری را نمی توان مستقیماً به کار گرفت و باید اصلاح شود و پارامتر چاپ آن باید بهینه شود تا با ویژگی ماده جدید مطابقت داشته باشد. هدف این مقاله یافتن پارامترهای بهینه (سرعت چاپ و ارتفاع لایه) بر اساس مواد قابل چاپ است. ماده جدیدی که قرار بود ساخته شود کامپوزیت پودر بیوسرامیک (هیدروکسی آپاتیت) و پلیمر (کلاژن) به شکل دوغاب با نسبت‌های ۹۹.۸٤ (w/v) % و ۰.۱٦ (w/v) %بود. در حالی که این چاپگر یک دستگاه چاپگر سه بعدی تجاری بود که در ظرف کارتریج و براکت آن تغییراتی ایجاد شده بود. پارامترهای چاپ ارتفاع لایه (۰.٦٥، ۱.۰، ۱.۳٥ میلی متر) و سرعت چاپ (۱٤.٤، ۲٥، ۳٥.٦ میلی متر در دقیقه) بود. بهینه سازی پارامتر چاپ با استفاده از روش سطح پاسخ (RSM) با ۱۳ مجموعه نمونه. نمونه‌های آزمایشی برای تعریف مواد قابل چاپ به شکل خط و به شکل مستطیل برای مطالعه موردی چاپ شدند. قابلیت چاپ به عنوان پاسخ به تنظیمات پارامتر بهینه بر اساس ٥٪ حداکثر خطای ابعاد نمونه چاپ شده در مقایسه با داده های -D ۳CAD تعریف شد. داده های به دست آمده با استفاده از آنالیز واریانس تجزیه و تحلیل شد. نتایج نشان می‌دهد که پارامتر چاپ راه‌اندازی بهینه به ترتیب ۱۰/۰۰۹ میلی‌متر در دقیقه برای سرعت چاپ و ۰/٥۰٥۰ میلی‌متر برای ارتفاع لایه بود که بعد خطای به‌دست‌آمده از آزمایش ۰/۰۱۳ میلی‌متر مربع (۰/٥۹ درصد) کمتر از خطای مجاز ٥ درصد بود. (۰.۱۲٥ میلی متر مربع).